Dynamic polarization in the Coulomb dissociation of ^{8}B

H. Esbensen[1] and G. F. Bertsch[2]
[1]*Physics Division, Argonne National Laboratory, Argonne, Illinois 60439*
[2]*Institute for Nuclear Theory, University of Washington, Seattle, Washington 98195*
(Received 8 July 2002; published 17 October 2002)

The Coulomb dissociation of ^{8}B on high-Z targets can be described by first-order perturbation theory at high beam energies but the far-field approximation, which is commonly used, becomes inaccurate at impact parameters less than $\sim$25 fm. The leading-order correction at lower beam energies is a dynamic polarization effect, which reduces the dissociation probability. The relative significance of the effect scales roughly as Z/E in terms of the target charge Z and beam energy E. The reduction due to a destructive Coulomb-nuclear interference, on the other hand, is rather modest.

DOI: 10.1103/PhysRevC.66.044609 PACS number(s): 24.10.−i, 25.60.−t, 25.70.De

We have investigated the Coulomb dissociation of ^{8}B in dynamical calculations that treat the $E0$, $E1$, and $E2$ fields of the target nucleus to all orders. Our purpose is to determine the influence of the dynamic polarization, which is the leading order correction to first-order perturbation theory at lower beam energies [1], and also to test the validity of the far-field approximation, which is commonly used in first-order calculations. The far-field approximation assumes that projectile and target do not overlap during the collision but that may be a poor approximation, as pointed out in Ref. [2], in particular for a weakly bound nucleus like ^{8}B.

The calculations we have performed are similar to those we presented for ^{17}F in Ref. [1], so we refer to that work for technical details. Basically, we describe the relative motion of projectile and target by classical Coulomb trajectories, whereas the relative motion of the valence proton and the ^{7}Be core is treated quantum mechanically by solving the time-dependent Schrödinger equation numerically.

The dynamic polarization effect can be isolated by repeating the dynamical calculations with opposite sign of the Coulomb form factors, i.e., by changing the sign of the target charge. From the two sets of dissociation probabilities $P_{\rm CD}^{(\pm)}(b)$, with positive and negative target charge, we define the Barkas factor

$$B=\frac{P_{\rm CD}^{(+)}-P_{\rm CD}^{(-)}}{P_{\rm CD}^{(+)}+P_{\rm CD}^{(-)}}, \tag{1}$$

which is a good measure of the dynamic polarization effect [1]. It is noted that the difference in the numerator depends on odd powers of Z (in a perturbation expansion of the probabilities), whereas the even power terms cancel. The Barkas factor is therefore, proportional to Z to leading order in the target charge. We shall use the parametrization

$$B=-\frac{Ze^2}{E}\,\frac{C}{\sqrt{b_{eff}^2+a^2}}\left(\frac{40}{E}\right)^{\nu}, \tag{2}$$

as we did in Ref. [1], to fit the dependence on beam energy E (in MeV/nucleon) and impact parameter b by adjusting the parameters C, a, and ν. The dependence on b in Eq. (2) is expressed through b_{eff}, which is the minimum projectile-target distance along a Coulomb trajectory.

The average dissociation probability for the two sets of target charges is compared to first-order perturbation theory, $P_{CD}^{(1)}$, by defining the ratio

$$A=\frac{P_{\rm CD}^{(+)}+P_{\rm CD}^{(-)}}{2P_{\rm CD}^{(1)}}. \tag{3}$$

The actual Coulomb dissociation probability (for positive target charge) is then given by

$$P_{CD}(b,E)=P_{CD}^{(1)}(b,E)A(1+B). \tag{4}$$

It is reduced compared to first-order perturbation theory, as we saw for ^{17}F [1]; the B factor is negative and the A factor is usually less than one (except at very low energies).

The first-order calculation was done using the commonly employed far-field approximation, in which the nuclear response is determined by the strengths of the multipole moments, $dB(E\lambda)/dE_x$, where E_x is the excitation energy. These are combined with the so-called orbital integrals, $S_{\lambda\mu}(E_x,b)$, computed for each Coulomb trajectory and characterized by the impact parameter b of the trajectory. In terms of these quantities, the dissociation probability for a given impact parameter b is [3]

$$P_{CD}^{(1)}(b)=\sum_{\lambda\mu}\left(\frac{4\pi Ze}{(2\lambda+1)\hbar}\right)^2 \times\int_{S_p}^{\infty}dE_x\,\frac{|S_{\lambda\mu}(E_x,b)|^2}{2\lambda+1}\,\frac{dB(E\lambda)}{dE_x}, \tag{5}$$

where the lower integration limit S_p is the proton separation energy.

The far-field approximation (5) may become unreliable for a weakly bound, proton-rich nucleus like ^{8}B because of the large spatial extent of the valence proton [2]. We saw indications of that in Ref. [1], where the A factor for the Coulomb dissociation of the ^{17}F ground state became strongly reduced compared to one at small impact parameters. Moreover, the reduction compared to one persisted out to much larger impact parameters when the excited $1/2^+$ halo state of ^{17}F was chosen as the initial state.

In this work we also compare the dynamical calculations to first-order calculations that treat the Coulomb multipole

fields from the target correctly, both for close and distant collisions. Such calculations can be tedious because one would have to calculate first-order matrix elements of the Coulomb fields for each point of the projectile-target trajectory. Instead of developing a new computer code to perform this task, we have modified our dynamical code, which solves the time-dependent Schrödinger equation numerically and treats the multipole fields correctly. Thus we have simply replaced the full wave function ψ in the source term associated with the Coulomb field, $V_{Coul}\ \psi$, by the wave function of the initial state. The A factors we obtain by employing this ''correct'' first-order calculation in Eq. (3) are much closer to one, as we shall see.

The nuclear-induced breakup may also become important when the far-field approximation for the Coulomb dissociation breaks down. However, it is not realistic to calculate the nuclear-induced breakup in first-order perturbation theory, as we demonstrated in Ref. [4]. We will therefore, consider the influence of the nuclear proton-target interaction only in full dynamical calculations. The nuclear interaction between the ^{7}Be core and the target will affect the breakup at small impact parameters but we will ignore it for convenience, as we did in Ref. [1].

All calculations are based on a simplified $^7\mathrm{Be}+p$ two-body model of ^{8}B, which we have developed [5] and applied [4] previously. It is based on the Coulomb interaction and a nuclear Woods-Saxon well [with parameters: $V_0=-47.72$ MeV, $R_0=2.391$ fm, $a=0.52$ fm]. The spin-orbit interaction is set to zero and the initial state is a p-wave bound by 137 keV. The dynamical calculations include all partial waves up to $l_{max}=5$, and radial wave functions are calculated on a grid up 70 fm with a step size of 0.2 fm.

We show in Fig. 1 the Coulomb dissociation probabilities we obtain for ^{8}B on a ^{58}Ni target as a function of beam energy. Results are shown at the three impact parameters indicated in the figure. The solid circles are the results of dynamical calculations with the (physical) positive target charge, whereas the diamonds are the results we obtain for the (unphysical) negative target charge. The two sets of results do not differ much at 40 MeV/nucleon but they differ substantially below 10 MeV/nucleon.

The solid curves in Fig. 1 are the results of first-order perturbation theory obtained in the far-field approximation. This is evidently a poor approximation at smaller impact parameters since it exceeds both dynamical calculations substantially. The dashed curves are the results of first-order calculations that employ the correct Coulomb form factors for close and distant collisions. They are seen to be in much better agreement with the average of the two sets of dynamical calculations. Roughly speaking, and as we discuss in more detail below, the difference between the full dynamical calculations and the correct first-order calculations is mainly caused by the dynamic polarization.

The Barkas factors extracted from dynamical calculations with a ^{58}Ni and a ^{208}Pb target are shown in Figs. 2(a) and 2(b), respectively, as functions of the impact parameter. Results are shown for different beam energies, which are indicated by the numbers (in MeV/nucleon). The solid curves show the parametrization (2) with $C=1.25$, $a=37$ fm, and

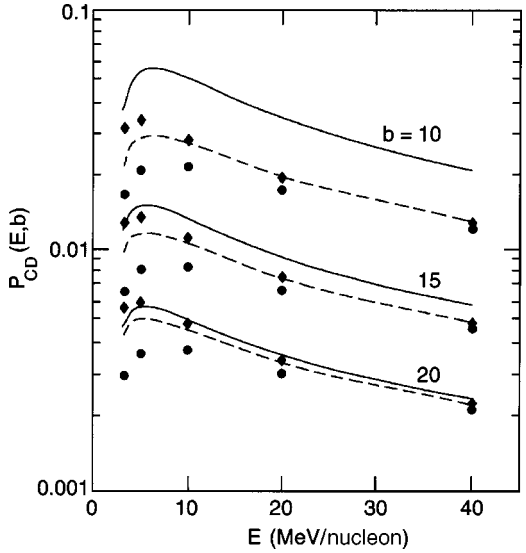

FIG. 1. Coulomb dissociation probabilities for ^{8}B on a ^{58}Ni target as functions of beam energy at the three impact parameters $b=10$, 15, and 20 fm. The dashed curves are the results of first-order perturbation theory. The solid curves are the first-order results obtained in the far-field approximation. The solid circles are dynamical results for a positive target charge ($Z=+28$); diamonds are for the negative target charge ($Z=-28$).

$\nu=0.07$. These parameters were determined by fitting the Barkas factors at 10, 20, and 40 MeV/nucleon on the ^{58}Ni target. They provide a fair prediction for the ^{208}Pb target at 20 and 40 MeV/nucleon, which confirms the expected Z dependence.

In Fig. 3 we show the impact parameter dependence of the A factors for the ^{58}Ni target. The left panel (a) shows the A factors we obtain when we employ the far-field approximation in the first-order calculation that appears in the denominator of Eq. (3). The results are shown in increasing order at 5, 10, 20, and 40 MeV/nucleon. They all show a dramatic falloff at smaller impact parameters. We saw a similar trend for ^{17}F in Ref. [1] and suggested that it was due to

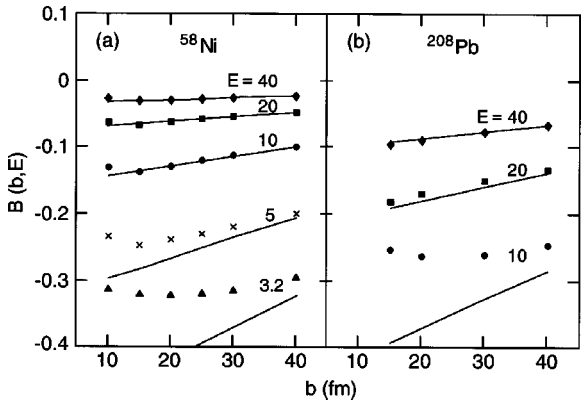

FIG. 2. Barkas factors [defined in Eq. (1)] for ^{8}B on ^{58}Ni (a) and ^{208}Pb (b) targets are shown as functions of the impact parameter. The beam energies (E in MeV/nucleon) are indicated in the figure. The solid curves show the parametrization of Eq. (2) with $C=1.25$, $a=37$ fm, and $\nu=0.07$.

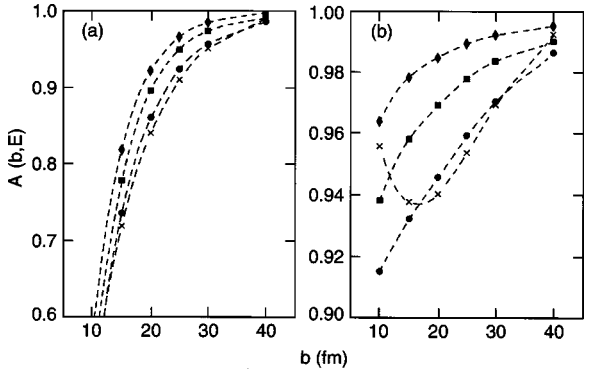

FIG. 3. *A* factors for ^{8}B on a ^{58}Ni target are shown as functions of impact parameter at the four beam energies of 5 (x), 10 (circles), 20 (squares), and 40 MeV/nucleon (diamonds). The results at a given energy are connected by dashed curves. Panel (a) shows the *A* factors one obtains from Eq. (3) when the first-order calculation is based on the far-field approximation. Panel (b) shows the *A* factors one obtains when the correct first-order calculation is employed in Eq. (3).

close collisions, which are treated correctly in the dynamical calculations but not in the first-order, far-field approximation. This interpretation is essentially confirmed in Fig. 3(b), which shows the *A* factors we obtain when we employ the correct first-order calculation in the denominator of Eq. (3). The reduction compared to one is now quite modest (note the different scale). The *A* factor at 5 MeV/nucleon has a somewhat irregular behavior as it starts to grow at the smallest impact parameters.

Let us now turn to the (^{8}B, ^{7}Be) breakup reaction that was measured at very low energy, namely, at about 3.22 MeV/nucleon on a ^{58}Ni target [6,7]. We have previously shown that higher-order effects are very large at the low energy of this experiment [4]. However, we did not separate the effects of close collisions and dynamic polarization. Moreover, we only considered the $\lambda=0$ to 2 multipole components of the proton-target nuclear interaction. It is therefore of interest to make a more detailed presentation. The data [7] are shown in Fig. 4 as function of the ^{8}B center-of-mass scattering angle. The curves labeled by letters are the results of various calculations. They were obtained simply by multiplying calculated probabilities with the Rutherford cross section.

Curve (a) in Fig. 4 shows the first-order Coulomb dissociation obtained in the far-field approximation. This curve is about 25% higher than was shown in Fig. 2 of Ref. [4], due to a numerical error in the previous calculation. Curve (b) is the correct first-order result which is based on the correct Coulomb form factors for close and distant collisions. The effect of close collisions is seen to cause a strong reduction at larger scattering angles; it sets in around 20°, which corresponds to an impact parameter of 25 fm.

The results of dynamical Coulomb dissociation calculations are shown by the dotted curve (c) in Fig. 4. They are reduced compared to curve (b) mainly because of the dynamic polarization effect, which is of the order of 30% [c.f. Fig. 2(a)]. The dynamic Coulomb dissociation is essentially identical to the result we obtained previously [4], and so is

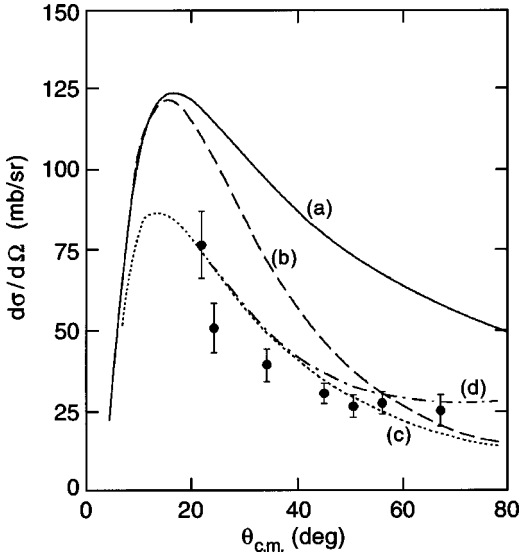

FIG. 4. Differential cross sections for the (^{8}B, ^{7}Be) reaction on a ^{58}Ni target at 3.22 MeV/nucleon, as functions of the ^{8}B center-of-mass scattering angle. The data are from Ref. [7]. The solid curve (a) shows the first-order Coulomb dissociation based on the far-field approximation. The dashed curve (b) is the correct first-order result, based on the correct form factors for close and distant collisions. The dotted curve (c) shows the dynamic Coulomb dissociation. The dotted-dashed curve (d) is the total (^{8}B, ^{7}Be) cross section obtained in dynamical calculations that include Coulomb fields and the nuclear proton-target interaction.

the result we obtain when we include the $\lambda=0$ to 2 multipole components of the proton-target nuclear interaction. The latter calculation shows a strong effect of a destructive Coulomb-nuclear interference as illustrated in Fig. 2 of Ref. [4].

An interesting and somewhat surprising feature is that the effect of the destructive Coulomb-nuclear interference essentially disappears when we include all multipole components of the nuclear interaction, i.e., $\lambda=0$ to $2l_{max}$, where $l_{max}=5$ is the maximum single-particle angular momentum that we consider in the calculations. Thus the diffraction dissociation we obtain is essentially indistinguishable from the dotted curve in Fig. 4. The only apparent effect of the nuclear proton-target interaction is the contribution from stripping reactions, which is included in the dotted-dashed curve (d) in Fig. 4. The absorption due to the core-target nuclear interaction should also set in at some point and reduce the (^{8}B, ^{7}Be) cross section but we will not consider that issue here.

It is instructive to see in more detail how close collisions affect the first-order $E1$ and $E2$ Coulomb dissociation. This is illustrated in Fig. 5 for the same target and beam energy as considered in Fig. 4. The solid curves are the results we obtain in the far-field approximation. The dashed curves are based on the correct form factors for close and distant collisions. The $E2$ component is seen to be affected the most. This is not so surprising because the far-field form factor, $\propto r^{\lambda}/r_{pt}^{\lambda+1}$, with r_{pt} the projectile-target separation, is weighted more strongly towards larger proton-core separations r for the quadrupole ($\lambda=2$) than for the dipole (λ

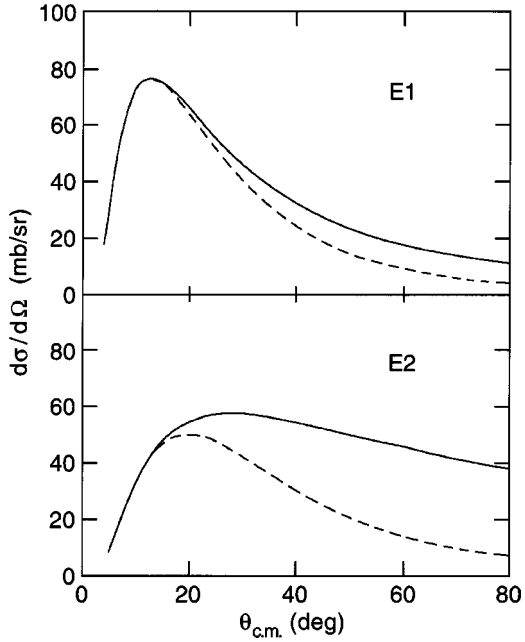

FIG. 5. Differential cross sections for the first-order $E1$ and $E2$ Coulomb dissociation of ^{8}B on a ^{58}Ni target at 3.22 MeV/nucleon, as functions of the ^{8}B center-of-mass scattering angle. The solid curves show the far-field approximation. The dashed curves are the correct first-order results, based on the correct form factors for close and distant collisions.

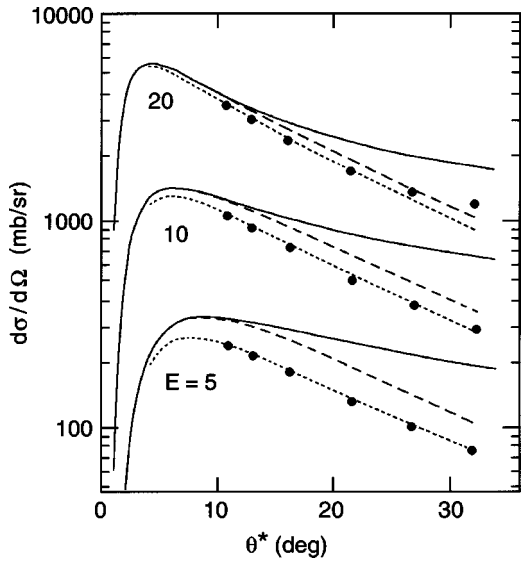

FIG. 6. Differential cross sections for the $^8\mathrm{B}\rightarrow{}^7\mathrm{Be}+p$ diffraction dissociation on a ^{58}Ni target, at $E=5$, 10, and 20 MeV/nucleon. The abscissa: $\theta^*=\theta_{\mathrm{c.m.}}\times E/(5\ \mathrm{MeV/nucleon})$ is the ^{8}B center-of-mass scattering angle $\theta_{\mathrm{c.m.}}$ scaled by the factor $E/(5\ \mathrm{MeV/nucleon})$. The solid curves are the first-order results obtained in the far-field approximation. The dashed curves are the correct first-order results. The dotted curves show the results for the dynamic Coulomb dissociation. The solid points are the diffraction dissociation obtained when the nuclear proton-target interaction is also included in the dynamical calculations.

$=1$) field. Thus, when the correct form factors are used for close collisions, namely $\propto r_{pt}^{\lambda}/r^{\lambda+1}$ when $r>r_{pt}$, there will be a larger effect for quadrupole than for dipole transitions. This feature may be related to the empirical finding that the continuum $E2$ strength of ^{8}B, which is seen in Coulomb dissociation experiments, is quenched compared to most model predictions [9].

To summarize our results for the $^8\mathrm{B}\rightarrow{}^7\mathrm{Be}+p$ dissociation on a ^{58}Ni target, we show in Fig. 6 the cross sections we obtain as a function of scaled scattering angle: $\theta^*=\theta_{\mathrm{c.m}}\times E/(5\ \mathrm{MeV/nucleon})$, where $\theta_{\mathrm{c.m.}}$ is the ^{8}B center-of-mass scattering angle and $E=5$, 10, and 20 MeV/nucleon are the beam energies that are considered. The solid curves show the first-order results obtained in the far-field approximation. The dashed curves are the correct first-order results. Comparing the two sets of curves, one clearly sees the importance of close collisions when $\theta^*\geqslant 13°$, i.e., for impact parameter smaller than $\sim$25 fm. The dynamic Coulomb dissociation cross sections are shown by the dotted curve. The reduction compared to the dashed curves is mainly caused by the dynamic polarization, which has the characteristic $1/E$ beam energy dependence. The influence of close collisions, on the other hand, appears to be rather independent of energy.

To complete the story, we have also considered the influence of the nuclear proton-target interaction [8], including all multipole components of the nuclear field. The results we obtain for diffraction dissociation are shown by the solid points in Fig. 6 (the results for stripping are not included here). The reduction compared to the dotted curves, caused by a destructive Coulomb-nuclear interference, is surprisingly small. This is consistent with the result discussed above in connection with Fig. 4, and also with the results we obtained for ^{17}F (cf. Fig. 6 of Ref. [1]). Thus we find it important to include all multipole components of the nuclear interaction; restricting them to $\lambda=0$ to 2 may cause a strong but unrealistic destructive Coulomb-nuclear interference.

This work was supported by the U.S. Department of Energy, Nuclear Physics Division, under Contract No. W-31-109-ENG-38, and Grant No. DE-FG03-00-ER-41132.

[1] H. Esbensen and G.F. Bertsch, Nucl. Phys. **A706**, 383 (2002).
[2] C.H. Dasso, S.M. Lenzi, and A. Vitturi, Nucl. Phys. **A639**, 635 (1998).
[3] K. Alder and A. Winther, *Electromagnetic Excitation* (North-Holland, Amsterdam, 1975).
[4] H. Esbensen and G.F. Bertsch, Phys. Rev. C **59**, 3240 (1999).
[5] H. Esbensen and G.F. Bertsch, Nucl. Phys. **A600**, 37 (1996).
[6] J. von Schwarzenberg *et al.* Phys. Rev. C **53**, R2598 (1996).
[7] V. Guimarães *et al.*, Phys. Rev. Lett. **84**, 1862 (2000).
[8] R.L. Varner *et al.*, Phys. Rep. **201**, 57 (1991).
[9] M. Gai and C.A. Bertulani, Phys. Rev. C **52**, 1706 (1995).